Interpretive Nonlinear Viscoelasticity: Dynamic Properties of Nylon 6, Nylon 66, and Nylon 12 Fibers

D. C. PREVORSEK, Y. D. KWON, and R. K. SHARMA, *Corporate Research Center, Allied Chemical Corporation, Morristown, New Jersey 07960*

Synopsis

Nonlinear response of nylon 6, nylon 66, and nylon 12 fibers to sinusoidal straining under relatively large strain amplitude is analyzed in terms of the changes in properties during the straining, i.e., the change in modulus, change in internal friction and change in structure which involves energy release or absorption in straining. Modulus generally increases with strain but it decreases with increase of strain amplitude, the effect of strain amplitude being largest with nylon 6 and smallest with nylon 66. Mechanical loss increase with the increase of strain amplitudes in nonlinear manner, and the magnitude of change is largest with nylon 66 and smallest with nylon 6. During the extension phase, structural change occurring in nylon 6 is predominantly an increase in order or orientation while that with nylon 66 is crack opening or cavitation. Various aspects of the experiments and analysis of the data are described in detail.

INTRODUCTION

When a polymeric specimen is subjected to a relatively large sinusoidal strain (stress), the resulting stress (strain) is not sinusoidal. The distortion can result from changes in modulus as function of strain (or phase angle θ) during the cycle and changes in the internal friction as function of strain (or phase angle θ) during the cycle. The determination of the relative contribution of these two effects requires the knowledge of specimen modulus and internal friction at each instant of the experiment.

In recent publications,[1,2] we described a method and apparatus which allow such an analysis. The analysis is based on an experiment which involves the superimposition of a small amplitude high-frequency sinusoidal strain on the large-amplitude low-frequency sinusoidal strain. The response to the high frequency strain is used to monitor the changes in the viscoelastic properties of the sample while it is subjected to a large-amplitude low-frequency cyclic strain.

The analysis showed that, in addition to the effects of strain, the stress responses show also a pronounced strain rate effect and effects associated with the reversible, strain-induced structural changes. The results reported before concerned only oriented nylon 6 fibers. In this article we examine the results obtained with nylon 6, nylon 66, and nylon 12 fibers.

Journal of Applied Polymer Science, Vol. 25, 2063–2104 (1980)

0021-8995/80/0025-2063$04.20

EXPERIMENTAL

Apparatus

The dynamic viscoelastic measurements were carried out using RJS model 167 high strain dynamic viscoelastometer (RJS Corp., Akron, OH). The apparatus has the capability of subjecting samples to (1) sinusoidal strain, (2) constant strain rate periodic deformation, and (3) the above (1) and (2) with superimposition of a high-frequency small-amplitude sinusoidal strain. These three experiments are required to analyze the deviations of the stress response from linear behavior in terms of (1) strain dependence of modulus and internal friction during the cycle, (2) strain rate dependence of modulus and internal friction during the cycle, and (3) reversible strain-induced structural changes during the cycle.

The experiments discussed here were carried out in the temperature range of 30 to 150°C, strain amplitude range of 0.3% to the strain amplitude leading to rupture which varies from material to material. The frequency of the large amplitude sinusoidal strain (fundamental strain) was 0.1 Hz, and the frequency of the small amplitude, high frequency sinusoidal strain (superimposed strain) was 25 Hz.

Procedure to Measure Steady State Properties

When a polymeric fiber is subjected to a cyclic deformation with a strain amplitude exceeding about 0.1%, its viscoelastic properties vary with the time during the experiment. The property change may be so fast during the initial period of the experiment that a measurement may not be possible during the first few minutes of testing. However, the rate of property change decreases with time and within a few hours a steady state is usually reached where the properties remain essentially constant indefinitely or almost to the time of rupture.

An interruption of the experiment accompanied by a reduction of the stress to zero also leads to a change in the properties of the fibers which is opposite to that occurring during the initial period of the experiment. The magnitude of changes in properties resulting from periodic deformation (mechanical conditioning) usually increases with increasing strain amplitude and increasing temperature of the experiment. Thus, it is impossible to derive a rule of thumb to estimate the extent of change under various conditions. This further complicates the experimental work. However, we found that it is possible to obtain reproducible results if the samples are first exposed to the largest strain amplitude at the highest temperature of the experiment. The measurements are then made at progressively smaller strain amplitudes and lower temperatures. If these samples are then reexamined under conditions involved in these experiments, including the highest strain amplitude and the highest temperature, the differences between the first run and the repeat are insignificant. If, however, the first experiment is conducted at the smallest strain amplitude and the lowest temperature, and then the sample is subjected to more severe deformation and temperature conditions, the repeat of the experiment at lowest strain amplitude and temperature would normally differ considerably from the initial run.

The results discussed in this article were all obtained using this procedure. The testing starts with the most severe conditions which are then gradually re-

duced to the lowest level of strain amplitude. When experiments are conducted as function of temperature, the conditioning is carried out at the highest temperature and the measurements are recorded during the cooling of the specimen. The samples are kept for about 30 min at a given temperature before the measurements are recorded.

The effect of mechanical and thermal conditioning on dynamic properties of fibers is of considerable theoretical and technological importance because it is related to the delayed fracture (i.e., fatigue) of the specimen subjected to large periodic deformations. We plan to discuss these phenomena in more detail in a subsequent publication. This article concerns primarily the measurements and analysis of the viscoelastic properties under steady-state conditions. The reference to mechanical conditioning is made solely to indicate the time dependence of viscoelastic properties under cyclic deformation with large strain amplitudes and problems of obtaining reproducible results.

Materials Investigated

All fibers investigated in this study were melt-spun monofilaments. The essentially unoriented but partially crystalline undrawn fibers were drawn to maximum and heat-set for about 2 sec under drawing tension. The drawing apparatus consisted of a feed roll and a draw roll assembly, a heated draw pin, and a plate heater. With all the fibers the pin and the heater temperatures were maintained at 80 ± 1°C, respectively. Fibers classified as fully drawn were drawn to maximum, i.e., further increases in draw ratio led to excessive fiber breakage during drawing. No attempts were made to optimize the drawing process. With the low-draw-ratio nylon 6 fiber, the draw ratio was arbitrarily chosen to be $3.0x$.

Before testing, the fibers were characterized by small- and wide-angle x-ray diffraction. The results are summarized in Tables I and II.

RESULTS AND DISCUSSIONS

Average Properties

Property Changes during Experiment: Mechanical Conditioning of Samples

With the strain amplitudes investigated in this study, the samples undergo significant dimensional, structural, and property changes during the experiments. In most cases the rate of these changes decreases with time, and within a few hours the samples reach a steady state and the properties remain practically unchanged over prolonged periods of time (i.e., a few days). The properties at these steady-state conditions are somewhat dependent on previous thermal and stress histories of the test specimen. One way to resolve this problem is to condition the samples, before testing, at the highest temperature and largest strain amplitude of the experiment. Testing of specimens so conditioned leads to reproducible results when testing is conducted at lower temperatures and or smaller strain amplitudes. In addition, the time to reach a steady state at each new experimental condition is much shorter (i.e., between 15 and 30 min).

Effects of mechanical conditioning on mechanical loss and dynamic modulus

TABLE I
X-Ray Characteristics of Nylon 6 and Nylon 66 Fibers

		Nylon 6 fully drawn	Nylon 6 low draw ratio (3x)	Nylon 66
Lateral order (%)	α	93	76	91
	β	1	3	1
	γ	0	7	
	amorphous	6	14	8
Crystallinity (%)	α	68	47	64.3
	β	1	1.8	0.7
	γ	0	4.3	
	amorphous	31	47	35.0
Crystallite size (Å)	α_1	44.8	47	43.9
	α_2	30.0	38	32.9
	β	52.3	50.7	61.4
d Spacing (Å)	α_1	4.39	4.38	4.34
	α_2	3.87	3.77	3.77
	β	8.26	8.18	8.30
Orientation function	f(α)	0.945	0.903	0.970
SAXS spacing (Å)		83	80	101

(defined as the ratio of stress–strain amplitudes) are shown in Figures 1 and 2.

Note that the conditioning time increases with decrease in strain amplitude from ~2 hr at 1.2% strain amplitude to ~6 hr at 0.8% strain amplitude. Since the change in properties during the conditioning may exceed 30%, it is obvious that this effect must not be neglected. With all polymeric samples investigated to date we observed without exception that the mechanical conditioning in cyclic tension leads to a decrease in the mechanical loss while the dynamic modulus

TABLE II
X-Ray Characteristics of Nylon 12 Fiber

Lateral order (%)	crystalline phase	76
	amorphous phase	24
Crystallinity (%)		67
Amorphous (%)		33
Crystallite size (Å)	(020)	105
	(011)	55
d-Spacing (A)	(020)	16
	(011)	4.12
Orientation function	(020)	0.883
	(011)	0.947
SAXS spacing (Å)		126.2

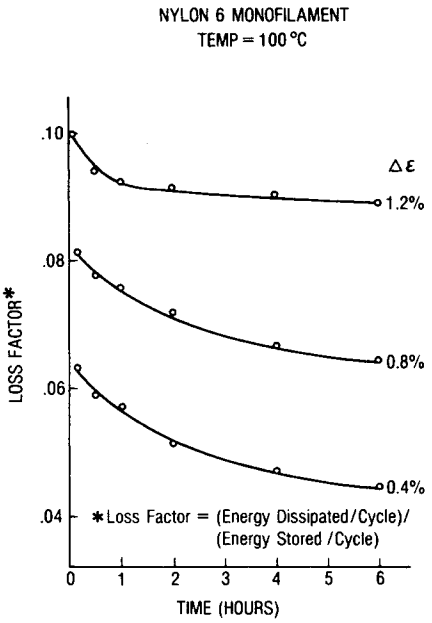

Fig. 1. Effect of mechanical conditioning on loss factor for nylon at 100°C. The loss factor is the energy dissipated per cycle per energy stored per cycle.

increases. Since these changes are accompanied by sample elongation (creep) they could be attributed to small increases in molecular orientation and crystallization.

In studying the effects of mechanical conditioning it is important to note that the changes in properties caused by conditioning are, to a large degree, reversible. That is, during a period of rest at zero tension, the properties change in the op-

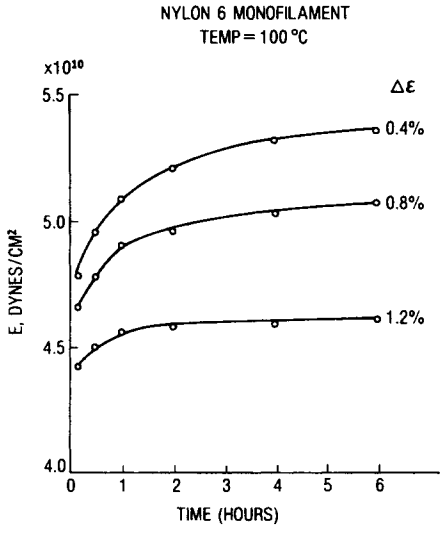

Fig. 2. Effect of mechanical conditioning on dynamic modulus for nylon 6 at 100°C.

posite direction to that occurring during conditioning. During the period of rest, the cords relax and the properties approach those of the original sample. However, the recovery is seldom complete and its extent depends on pretension. The pertinent data on the effect of the rest period on viscoelastic properties of nylon 6 cords are shown in Figures 3 and 4.

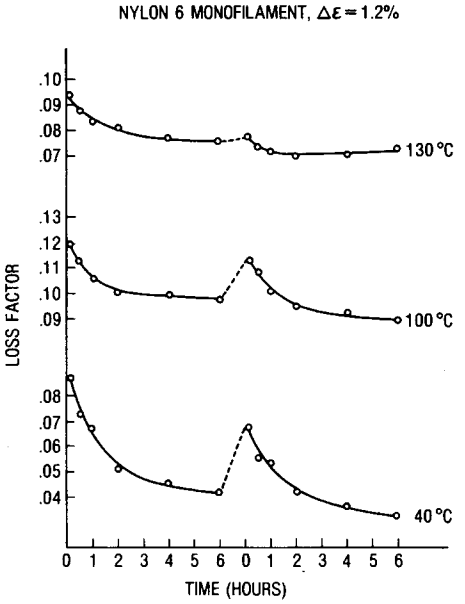

Fig. 3. Effect of rest period on loss factor during mechanical conditioning for nylon 6, $\Delta\epsilon = 1.2\%$; (- - -) rest period at relaxed state.

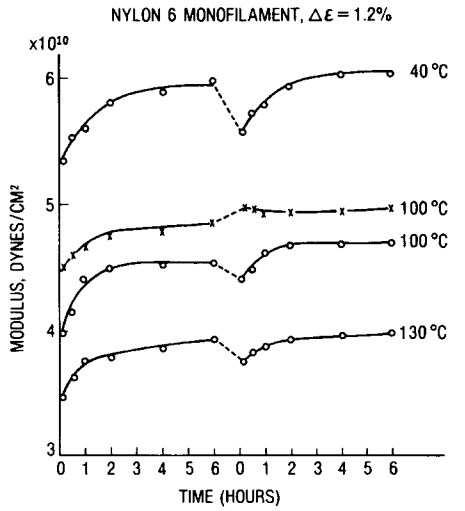

Fig. 4. Effect of rest period on modulus during mechanical conditioning for nylon 6, $\Delta\epsilon = 1.2\%$; (- - -) rest period at relaxed state; (x- - -x) at stretched state.

Steady-State Properties

The plots of mechanical loss as function of temperature and strain amplitude are presented in Figures 5(a)–5(d). The mechanical loss has a well-defined maximum at ~90, ~80, and ~100°C for fully drawn nylon 6, nylon 12, and nylon 66 fibers, respectively. The temperature of maximum loss increases with increasing orientation (draw ratio) as indicated by the data of low- and high-draw-ratio nylon 6 fibers. With the low-draw-ratio fiber, the maximum loss appears at ~75°C which is ~15°C below the temperature of maximum loss with the fully drawn nylon 6 fiber. Since the loss maxima indicate the T_g of the fibers, a large decrease in modulus is expected in the temperature interval about the temperature of maximum loss. This trend is observed with all four fibers as it can be seen in Figures 6(a)–6(d) where the modulus data are presented.

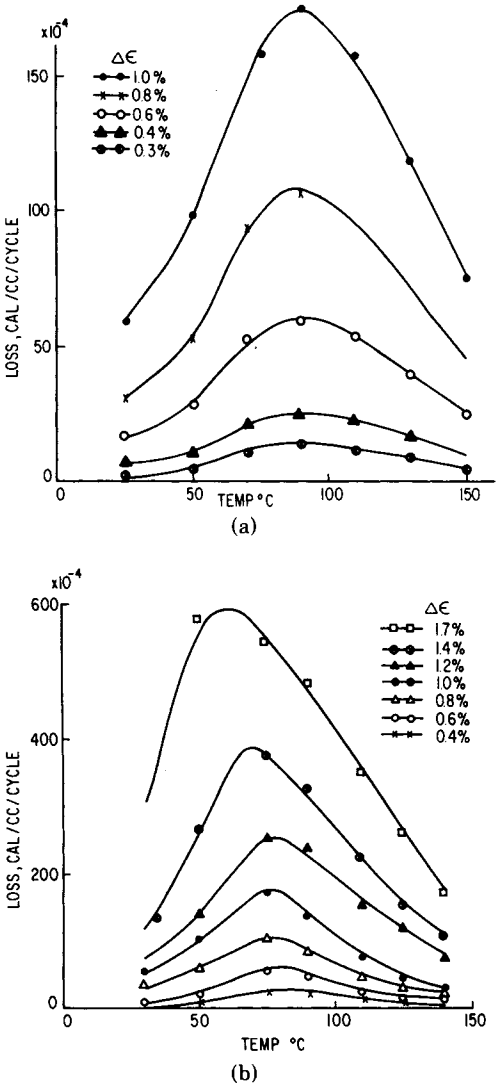

Fig. 5. Mechanical loss. (a) nylon 6, 5x, (b) nylon 6, 3x, (c) nylon 66, (d) nylon 12.

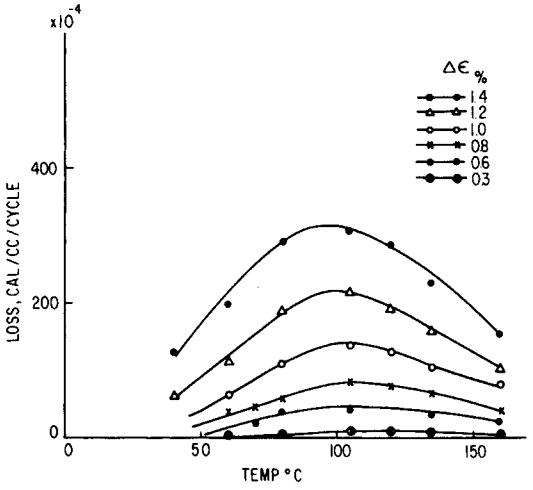

(c)

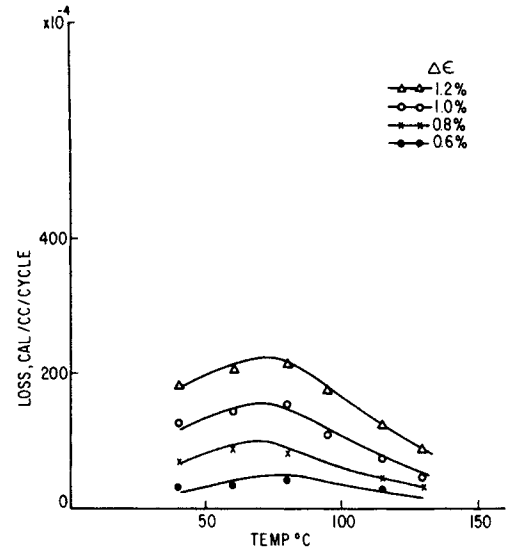

(d)

Fig. 5. (*Continued from previous page.*)

Based on the above results it can be concluded that under large-amplitude sinusoidal strains the changes in modulus and mechanical loss with the temperature follow very closely the behavior of fibers under small strain amplitudes, i.e., in linear viscoelastic experiments. However, the deviation from linear behavior can be readily observed and expressed in quantitative terms when modulus or mechanical loss is plotted against strain amplitude. Note that with linear viscoelastic materials, the dynamic modulus is independent of strain amplitude and the loss is proportional to the square of strain amplitude.

Plots of log(loss) vs. log($\Delta\epsilon$) in Figures 7(a)–7(d) show that with all four fibers the lines are nearly straight but the slope is significantly larger than 2.

Of particular interest is the slope $d(\text{loss})/d(\Delta\epsilon)^2$ which can be used as an index

of nonlinearity in the loss. In Tables III–VI values of $d(\text{loss}/d(\Delta\epsilon)^2$ for various temperatures and strain amplitudes are presented. As expected, $d(\text{loss})/d(\Delta\epsilon)^2$ increases with increasing strain amplitude. When $d(\text{loss})d(\Delta\epsilon)^2$ at a given strain amplitude is plotted as function of temperature, we observed a minimum near the glass transition temperature of these fibers. Also interesting is the index for nonlinearity in mechanical loss, R, defined by

$$R = \frac{[d(\text{loss})/d(\Delta\epsilon)^2]_{\text{exp}}}{[d(\text{loss})/d(\Delta\epsilon)^2]_{\text{linear}}}$$

where $[\ ]_{\text{exp}}$ is the experimental value of the slope and $[\ ]_{\text{linear}}$ is the calculated value of slope assuming linear behavior.

At a given strain amplitude, e.g., $\Delta\epsilon = 1.0\%$, the lowest values are found with nylon 12 (1.15–1.63), the highest with nylon 66 (1.33–4.19). In the same temperature interval, the values of $d(\text{loss})/d(\Delta\epsilon)^2$ are lower with nylon 6 than nylon 66. Plots of the above-mentioned slope ratio for fully drawn nylon 6, nylon 66, and nylon 12 are presented in Figures 8(a)–8(e). Note the large difference between the behavior of nylon 66 as compared with nylon 6 and nylon 12 at temperatures below and above the glass transition temperature of these fibers.

The examination of the slope $d\text{E}/d\Delta\epsilon$, i.e., rate of change in the dynamic modulus with $\Delta\epsilon$, for various fibers shows that this slope is always negative [see Figs. 9(a)–9(d)]. With a few exceptions, the absolute value of slope $|dE/d\Delta\epsilon|$ decreases with increasing temperature and decreasing modulus. The most comprehensive data of E vs. $\Delta\epsilon$ are those of fully drawn nylon 6. These data show that $|dE/d\Delta\epsilon|$ is not constant but increases from zero at very small strains and reaches its maximum at about $\Delta\epsilon \approx 0.5\%$ and then decreases to a value of about 1.0–1.3 at strain amplitudes between $\Delta\epsilon = 0.8\%$ and $\Delta\epsilon = 1.0\%$.

The comparison of data of low- and high-modulus nylon 6 fibers show that, with fibers of same chemical composition but different orientation and modulus, $|dE/d\Delta\epsilon|$ decreases with decreasing orientation and modulus.

The results above are consistent with the effect of modulus (i.e., stress) on the magnitude of $|dE/d\Delta\epsilon|$. Thus it appears that the lowering of the modulus with strain amplitude is primarily a result of sample dilation under cyclic loading, which in turn is a function of average sample stress during the cycle.

The comparison of plots of E vs. $\Delta\epsilon$ for the three fully drawn fibers in the $\Delta\epsilon$ range of 1.0% shows that $|dE/d\Delta\epsilon|$ is largest for nylon 6 and lowest for nylon 66, with the nylon 12 showing the largest variations.

These data reveal interesting differences between the reponses of these fibers at large sinusoidal strain amplitudes, with nylon 6 showing a much larger sensitivity in modulus to increases in strain amplitude than nylon 66. The opposite trend, namely, nylon 66 showing a larger sensitivity to increase in strain amplitude than nylon 6, is observed when the loss is examined as function of strain amplitude.

The hypothesis that decrease in modulus results from the sample dilation is supported also by the plots of temperature of maximum loss versus strain amplitude (not shown). Since these plots indicate the effects of strain amplitude on the T_g of fiber, it can be assumed that a lowering (increase) in T_g suggests a lowering (increase) in specimen density.

In all the fibers investigated, we observed a significant decrease in the temperature of maximum loss (T_g) with increasing strain amplitude. To estimate

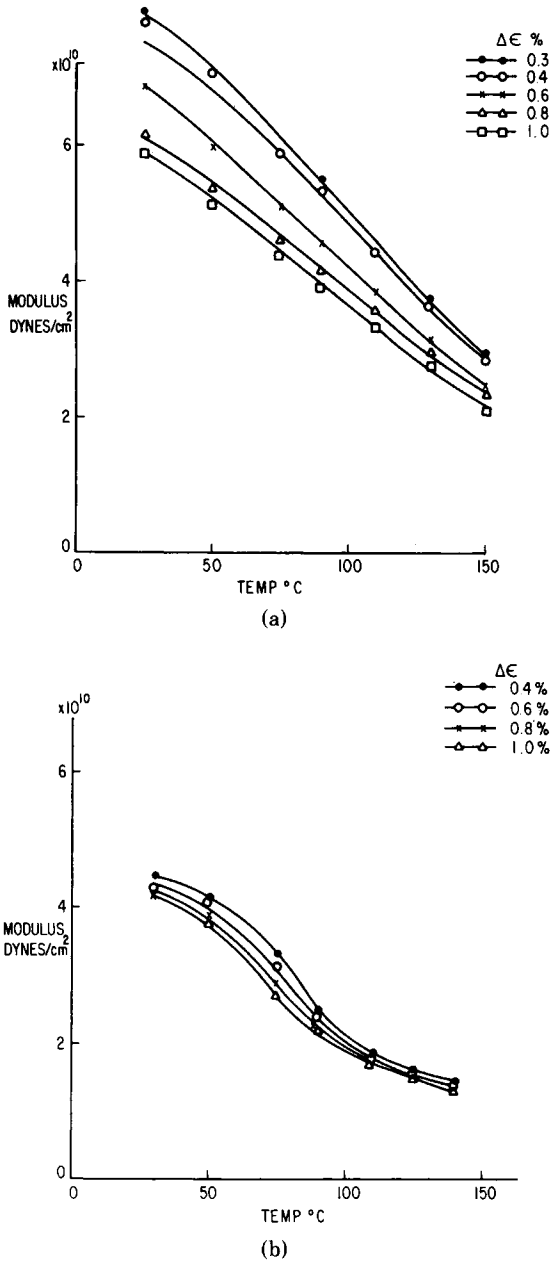

Fig. 6. Modulus, (a) nylon 6, 5x, (b) nylon 6, 3x, (c) nylon 66, (d) nylon 12.

the rate of change in T_g with strain amplitude more accurately, we carried out a series of experiments in which the viscoelastic measurements were carried out at 2°C intervals in the T_g region. From these data, the temperature of maximum loss could be determined with more precision than is possible from Figures 5(a)–5(d). Each of these temperatures was then corrected for the effect of self-heating of the filament resulting from hysteretic loss using a procedure to

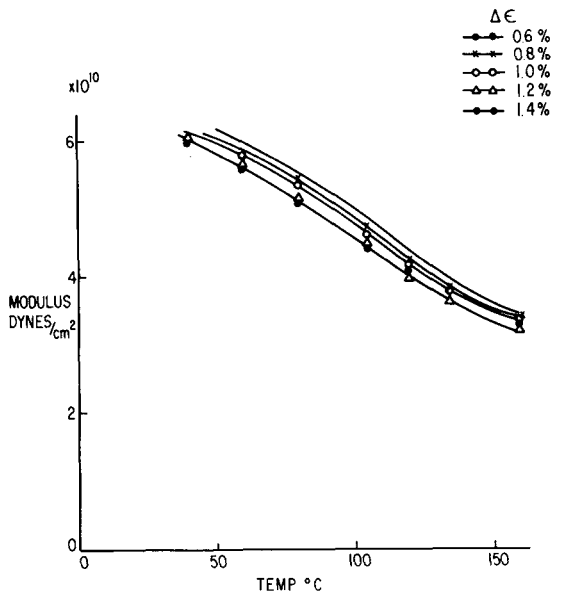

(c)

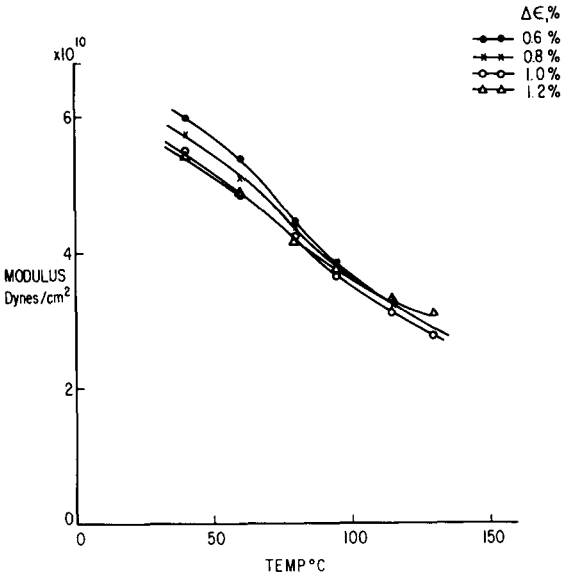

(d)

Fig. 6. *(Continued from previous page.)*

be described elsewhere. Such corrections ranged from about 1°C at the lowest strain amplitude to about 5°C at the highest amplitude. In the $\Delta\epsilon$ value between 0.6 and 1.2%, the change in T_g with percent strain amplitude ($dT_g/d\Delta\epsilon$) is about -11°C/% for the fully drawn nylon 6, -19.5°C/% for nylon 66, and -11.5°C/% for nylon 12. With the low-draw-ratio nylon 6, $dT_g/d\Delta\epsilon$ is about -23°C/%.

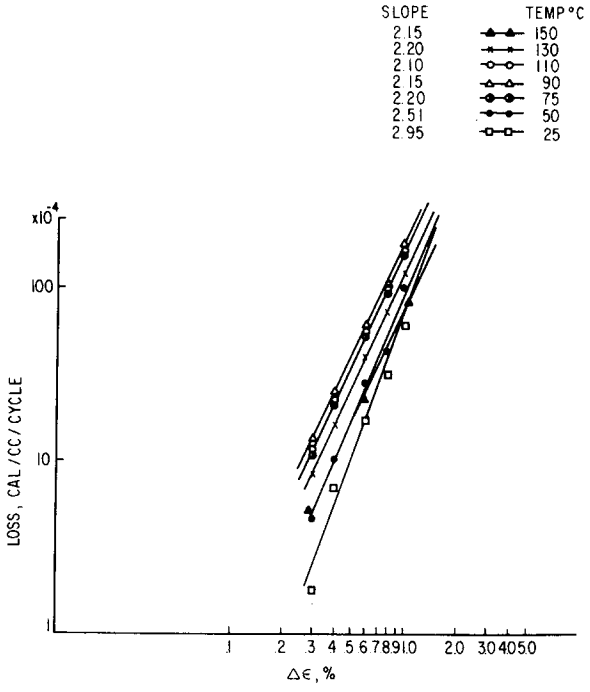

(a)

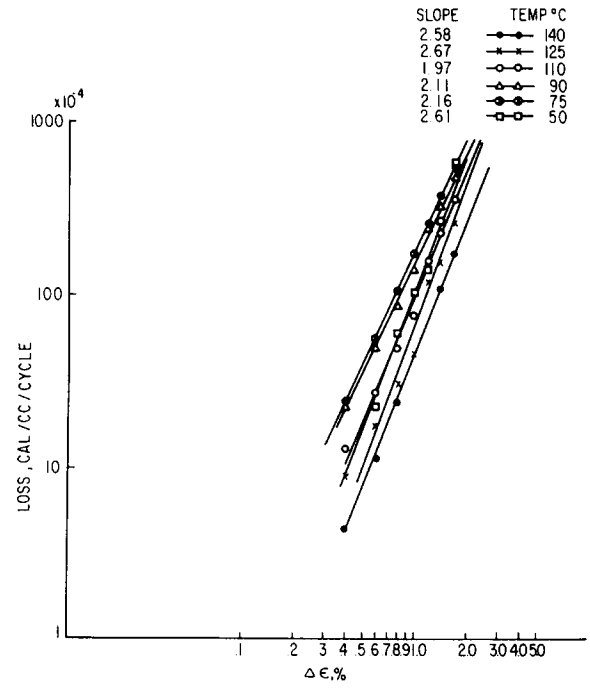

(b)

Fig. 7. Loss vs. $\Delta\epsilon$, (a) nylon 6, $5x$, (b) nylon 6, $3x$, (c) nylon 66, (d) nylon 12.

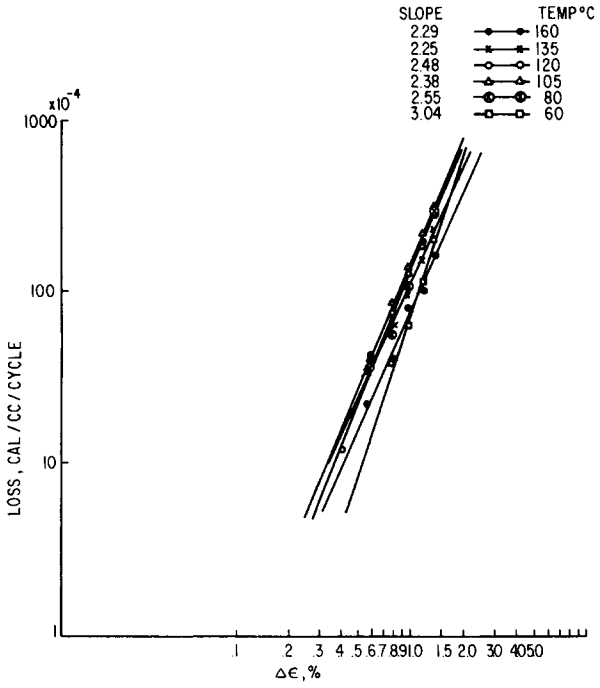

(c)

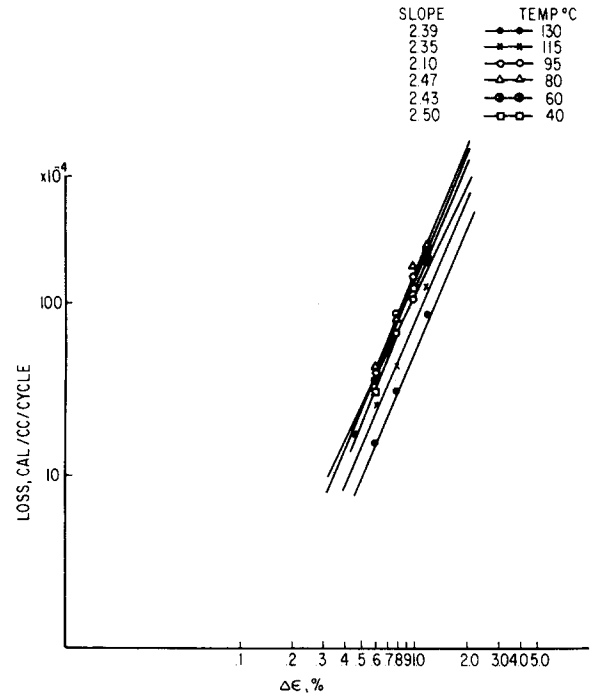

(d)

Fig. 7. (*Continued from previous page.*)

TABLE III
Slope $d(\text{loss})/d(\Delta\epsilon)^2$ and Ratio of the Actual Slope to the Slope Based on Linear Behavior, Nylon 6, 5x

T (°C)	Strain amplitude S_{linear}	0.3%		0.4%		0.6%		0.8%		1.0%	
		Sd[a]	R	Sd	R	Sd	R	Sd	R	Sd	R
25	20	22	1.10	50	2.50	50	2.5	60	3.00	100	5.00
50	52	56	1.08	85	1.63	90	1.73	110	2.11	120	2.31
75	120	122	1.02	150	1.25	150	1.25	165	1.32	175	1.40
90	150	155	1.03	160	1.07	170	1.13	180	1.20	200	1.33
110	125	127	1.02	155	1.24	155	1.24	160	1.28	165	1.32
130	90	91	1.01	110	1.20	110	1.20	110	1.22	120	1.33
150	53	56	1.06	70	1.32	70	1.32	75	1.40	80	1.51

[a] Sd: data slope.

TABLE IV

Slope $d(\text{loss})/d(\Delta\epsilon)^2$ and Ratio of the Actual Slope to the Slope Based on Linear Behavior, Nylon 6, 3x

T (°C)	Strain amplitude S_{linear}	0.4%		0.6%		0.8%		1.0%		1.4%		1.7%	
		Sd	R	Sd	R	Sd	R	Sd	R	Sd	R	Sd	R
50	56.2												
75	151	151	1.0	190	1.26	180	1.19	205	1.36	210	1.39	210	1.39
90	142.5	137.5	0.96	137.5	0.96	130	0.91	147.5	1.04	152.5	1.07	175	1.23
110	81.3	78	0.96	78	0.96	78	0.96	117.5	1.45	142.5	1.75	142	1.75
125	53.8	50	0.93	50	0.93	50	0.93	82	1.52	117.5	2.18	122.5	2.28
140	27.5	28.1	1.02	45	1.63	55	2.00	67	2.44	67.5	2.45	72	2.02

TABLE V
Slope $d(\text{loss}/d(\Delta\epsilon)^2$ and Ratio of the Actual Slope to the Slope Based on Linear Behavior, Nylon 66

T (°C)	Strain amplitude S_{linear}	$\Delta\epsilon$ 0.6%		0.8%		1.0%		1.2%		1.4%	
		Sd	R	Sd	R	Sd	R	Sd	R	Sd	R
60	22.2	60	2.70	76.8	3.45	93	4.19	140	6.31	168	7.57
80	44.4	106.7	2.40	125	2.82	143	3.22	160	3.60	205	4.62
105	102.4	126	1.23	148	1.45	162	1.58	178	1.74	184	1.80
120	108.2	116	1.07	130	1.20	144	1.33	166	1.53	184	1.70
135	93.3	100	1.07	108	1.16	116	1.24	130	1.39	136	1.46
160	38.9	62	1.59	73.3	1.88	76	1.95	92	2.37	96	2.48

TABLE VI
Slope $d(\text{loss})/d(\Delta\epsilon)^2$ and Ratio of the Actual Slope to the Slope Based on Linear Behavior, Nylon 12

T (°C)	Strain Amplitude S_{linear}	0.6%		0.8%		1.0%		1.2%	
		Sd	R	Sd	R	Sd	R	Sd	R
40	87.5	110	1.26	136.7	1.56	140.0	1.60	145	1.66
60	102.8	133.3	1.30	146.7	1.43	147.5	1.44	147.5	1.44
80	122.2	126.7	1.04	150.0	1.23	165	1.35	170	1.39
95	110.6	106.7	0.96	103.3	0.93	127.5	1.15	162.5	1.47
115	72.3	67	0.93	80	1.11	96.8	1.34	108.8	1.50
130	42.9	46.7	1.09	58.3	1.36	70	1.63	75	1.75

Analysis of Property Changes During the Cycle

Interpretive Nonlinear Viscoelasticity

The purpose of the interpretive viscoelastic analysis is to establish factors that are responsible for the deviations from the linear viscoelastic response. One manifestation of the nonlinearity is the distortion of the stress–strain hysteresis loop. The loop, which is elliptical with linear viscoelastic solids, can assume all kinds of distorted shapes if the materials exhibit nonlinear behavior.

The nonlinear response in cyclic deformation can be analyzed by means of harmonic analysis (see ref. 3). We investigated the use of the harmonic analysis to establish the causes for the deviation from the linear response. However, we were unable to relate the Fourier coefficients to the nonlinearity in elastic and viscous responses in a rational way.

The analysis, whose principles were discussed in detail elsewhere,[2] is based on the results of three viscoelastic experiments: (1) a fundamental large-amplitude sinusoidal strain experiment; (2) a constant strain rate cyclic deformation experiment of same frequency and same strain amplitude as in (1); and (3) experiments (1) and (2) with superimposition of a high-frequency small-amplitude sinusoidal strain.

The purpose of the constant rate deformation experiment is to eliminate the effects of deformation rate, while the purpose of superimposed strain is to follow up the changes in the viscoelastic properties during the fundamental large-amplitude sinusoidal strain experiment and constant strain rate periodic deformation experiment.

We proposed[2] that the changes in internal friction during the cycle can be expressed by the variation of the phase angle difference $\delta(\theta)$ with θ, and similarly the change in modulus can be represented by the variation of $E(\theta)$ with θ.

If we denote the storage modulus in linear viscoelasticity by E', and, for convenience put $\sigma_0 = 0$ in eq. (2) of ref. 2, it can be shown that the viscoelastic response to sinusoidal straining can be given by

$$\sigma(\theta) = (1/\cos\delta)\,\sigma_{\text{el}}\,(\theta + \delta) \tag{1}$$

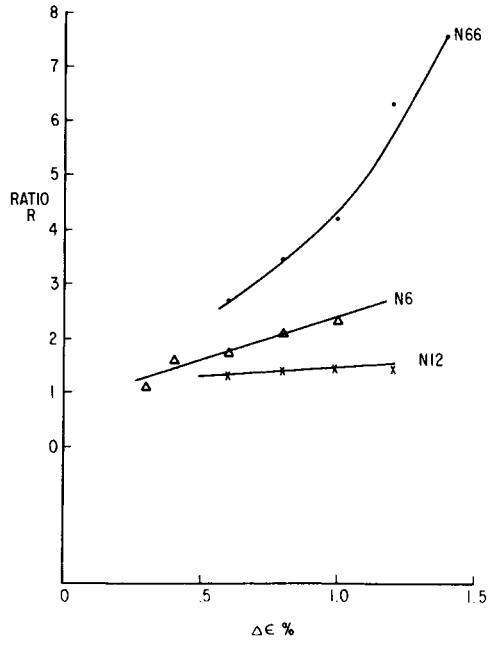

(a)

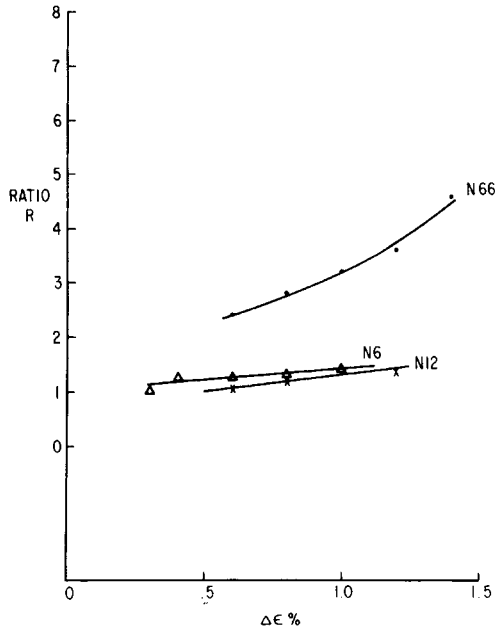

(b)

Fig. 8. Plot of ratio $R = [d(\text{loss})/d(\Delta\epsilon)^2]_{\text{exp}}/[d(\text{loss})/d(\Delta\epsilon)^2]_{\text{linear}}$ vs. $\Delta\epsilon$. (a) 60°C, (b) 80°C, (c) 115°C, (d) 130°C, (e) 150°C.

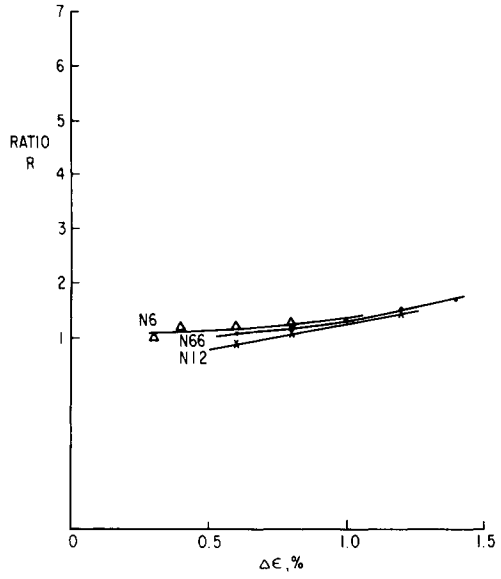

(c)

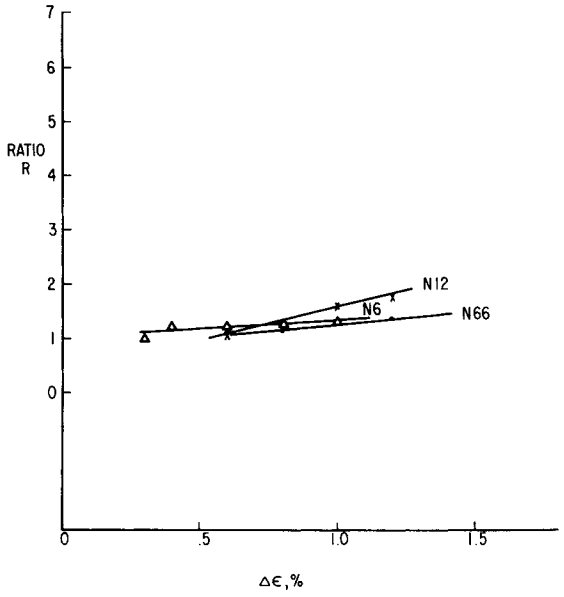

(d)

Fig. 8. (*Continued from previous page.*)

with

$$\sigma_{el}(\theta) = E'\Delta\epsilon \sin\theta \tag{2}$$

σ_{el} can be regarded as the elastic response. Equation (1) gives the viscoelastic response in terms of the elastic response.

We want to take a similar approach and express the nonlinear viscoelastic response in terms of the nonlinear elastic response $\sigma_{el}(\theta)$.

The procedure to estimate the nonlinear elastic stress, $\sigma_{el}(\theta)$ and $\delta(\theta)$ is described in detail in ref. 2.

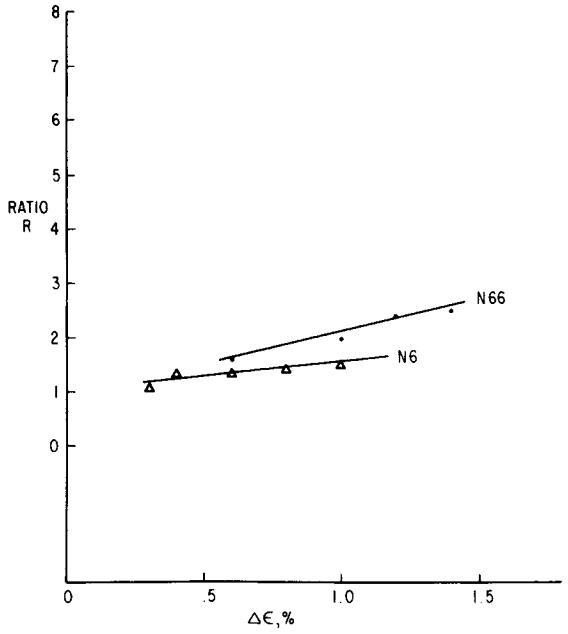

(e)

Fig. 8. (*Continued from previous page.*)

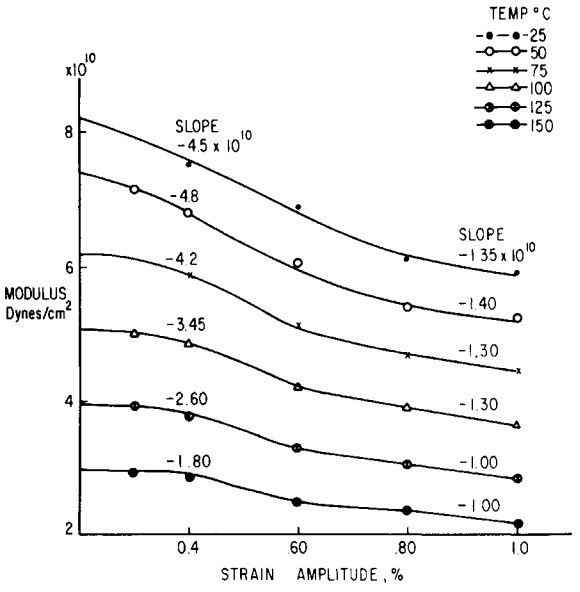

(a)

Fig. 9. Modulus vs. $\Delta\epsilon$, (a) nylon 6, $5x$, (b) nylon 6, $3x$, (c) nylon 66, (d) nylon 12.

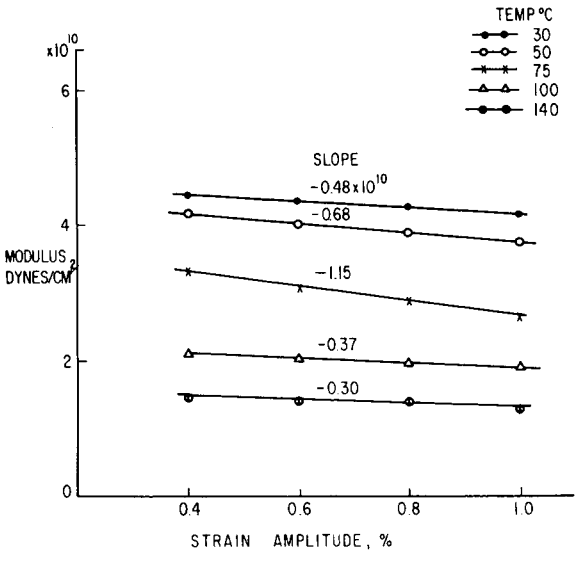

(b)

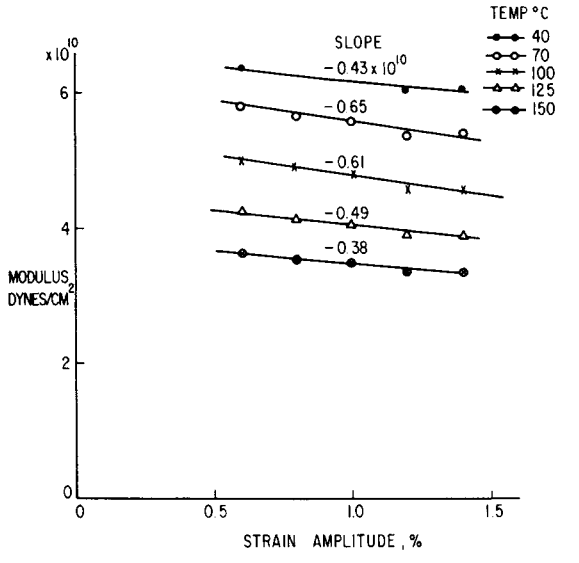

(c)

Fig. 9. (*Continued from previous page.*)

In the calculations, we assume that

$$E(\theta) = k(\Delta\sigma_s/\Delta\epsilon_s)_\theta \tag{3}$$

where $\Delta\sigma_s$ and $\Delta\epsilon_s$ are, respectively, the stress and strain amplitudes of the superimposed strain. The proportionality constant k is determined by means of

$$k(\Delta\sigma_s/\Delta\epsilon_s) = (d\sigma_{el}/d\epsilon)_\theta \tag{4}$$

and equating the observed stress amplitude of the fundamental stress response with the stress amplitude calculated using

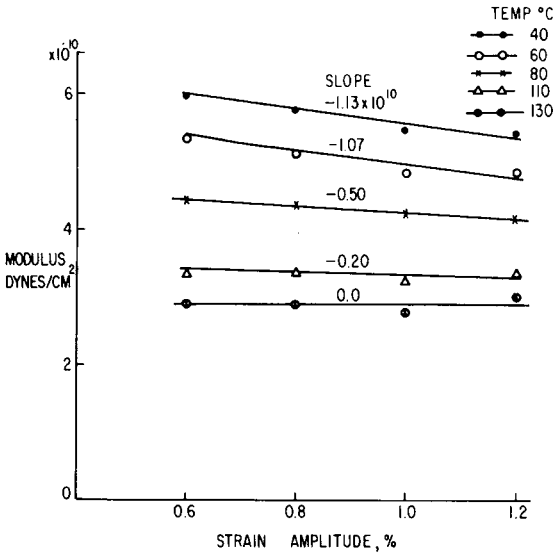

(d)

Fig. 9. (*Continued from previous page.*)

$$(\sigma_{max} - \sigma_{min}) = \int_{3\pi/2}^{\pi/2} E(\theta)\Delta\epsilon \cos\theta \, d\theta \tag{5}$$

Here $\Delta\epsilon$ is the fundamental strain amplitude, σ_{max} and σ_{min} are respectively the maximum and minimum stress as during the cycle, and $E(\theta)$ is as defined in eq. (3) (see Appendix A on k).

Equation (5) allows the calculation of the elastic stress response of a body whose $E(\theta)$ equals that of the material without mechanical loss:

$$\sigma_{el}(\theta) = \sigma_{min} + \int_{3\pi/2}^{\theta} E(\theta)\Delta\epsilon \cos\theta \, d\theta \tag{6}$$

A numerical example of the calculation of $\sigma_{el}(\theta)$ from $E(\theta)$ is shown in Appendix B.

Equation (5) involves a small error in the left-hand side term $(\sigma_{max} - \sigma_{min})$ which assumes that the difference between the maximum and minimum stresses for the elastic response equals that for the viscoelastic material in consideration. In general, the former should be smaller than the latter, i.e.,

$$(\sigma_{el\ max} - \sigma_{el\ min}) < (\sigma_{exp\ max} - \sigma_{exp\ min}) \tag{7}$$

In Appendix C we show that the difference in the maximum and minimum elastic stresses for a nonlinear viscoelastic solid can be approximated by

$$\Delta\sigma_{el} = \Delta\sigma_{exp} \cos\delta(90°) \tag{8}$$

with an error of less than 1%. Here, $\Delta\sigma_{el}$ is the difference between minimum and maximum elastic stress during the cycle, $\Delta\sigma_{exp}$ is the difference between maximum and minimum stress measured experimentally, and $\delta(90°)$ is the phase angle difference between the elastic and viscoelastic stress at $\theta = 90°$.

Changes in Modulus During the Cycle

The calculation of changes in elastic modulus during the cycle show that in all cases the modulus increases with increasing strain during the cycle.

At low strain amplitudes, $E(\theta)$ can sometimes be approximated, with a relatively small error, by a sinusoidal approximation

$$E(\theta) = E_0 + \Delta E \sin \theta \tag{9}$$

This implies a linear relationship between modulus and sample strain during the cycle. With increasing strain amplitude, eq. (9) becomes less accurate and the $E(\theta)$ must be represented by other means such as Fourier series.

Results of such a representation are shown in Table VII for the low-draw-ratio nylon 6 fiber. Note that the values of higher harmonics decrease much more rapidly with the strain amplitude of 0.4% than with the amplitude of 1.7%.

The changes in modulus with strain during the cycle can be characterized in terms of (1) values of the high-frequency modulus at $\theta = 0°$, $E(0)$; (2) difference between maximum and minimum values of the high-frequency modulus during the cycle

$$E_{\max} - E_{\min} = E(90°) - E(270°) = 2\Delta E' \tag{10}$$

(3) average rate of modulus increase with strain $\Delta E'/\Delta\epsilon$, where $\Delta\epsilon$ is the strain amplitude. In the quantities defined above, the high-frequency modulus equals the modulus as determined by the high-frequency small-amplitude superimposed strain. Note also that in the case where $E(\theta)$ can be represented by eq. (9), $E(0)$ is the average high-frequency modulus during a cycle and

$$\Delta E' = \Delta E \tag{11}$$

as defined in the eq. (10).

Values of $E(0)$, $\Delta E'$, and $\Delta E'/\Delta\epsilon$ obtained from the analysis of the strain superimposition experiments are summarized in Tables VIII–XI. The data indicate the following trends: $E(0)$ and $\Delta E'/\Delta\epsilon$ decrease with increasing temperature and increasing strain amplitude. In this respect there is an obvious

TABLE VII
Harmonic Analysis of $E(\theta)$

A_n or B_n dyn/cm^2	Nylon 6, 3x 31°C, $\Delta\epsilon$ = 1.7%[b]	Nylon 6, 3x 31°C, $\Delta\epsilon$ = 0.4%[b]
A_0	4.25×10^{10}	4.76×10^{10}
A_1	4.32×10^{8}	-1.48×10^{8}
A_2	2.02×10^{9}	1.18×10^{8}
A_3	1.87×10^{8}	-6.19×10^{6}
A_4	-1.36×10^{8}	-1.40×10^{7}
B_0	0	0
B_1	6.74×10^{9}	1.33×10^{9}
B_2	7.99×10^{7}	1.20×10^{7}
B_3	-6.18×10^{8}	-3.49×10^{7}
B_4	-2.51×10^{6}	1.94×10^{7}

[a] $E(\theta) = \sum_{n=0}^{\infty} A_n \cos n\theta + B_n \sin n\theta$.

[b] $\Delta\epsilon$ is the strain amplitude of the fundamental strain.

TABLE VIII
Values of E_0 and $\Delta E'$ (in 10^{10} dyn/cm^2) and $\Delta E'/\Delta\epsilon$ Nylon 6, 5x Monofil

Temperature (°C)	$\Delta\epsilon$(%) 1.0			0.8			0.6			0.4			0.3		
	E_0	$\Delta E'$	$\Delta E'/\Delta\epsilon$ ($\times 10^2$)	E_0	$\Delta E'$	$\Delta E'/\Delta\epsilon$ ($\times 10^2$)	E_0	$\Delta E'$	$\Delta E'/\Delta\epsilon$ ($\times 10^2$)	E_0	$\Delta E'$	$\Delta E'/\Delta\epsilon$ ($\times 10^2$)	E_0	$\Delta E'$	$\Delta E'/\Delta\epsilon$ ($\times 10^2$)
25	7.06	1.24	1.24	7.25	1.03	1.28	7.38	0.81	1.35	7.97	0.51	1.28	8.25	0.38	1.26
50	6.81	1.10	1.10	6.90	0.88	1.10	7.04	0.70	1.17	7.63	0.51	1.28	7.75	0.45	1.50
75	6.44	0.96	0.96	6.50	0.73	0.91	6.59	0.58	0.97	6.81	0.48	1.20	7.00	0.46	1.53
90	5.88	0.87	0.87	5.92	0.68	0.85	5.96	0.54	0.90	6.27	0.45	1.12	6.40	0.41	1.36
110	4.92	0.79	0.79	5.00	0.65	0.81	5.14	0.51	0.85	5.36	0.40	1.00	5.60	0.37	1.23
130	4.30	0.74	0.74	4.31	0.62	0.78	4.32	0.48	0.80	4.74	0.40	1.00	5.20	0.37	1.23
150	3.85	0.71	0.71	3.85	0.59	0.74	3.86	0.47	0.78	4.40	0.40	1.00	4.75	0.37	1.23

TABLE IX

Values of E_0 and $\Delta E'$ (in 10^{10} dyn/cm^2) and $\Delta E'/\Delta\epsilon$, Nylon 6, 3x Monofil

Temperature (°C)	$\Delta\epsilon$ (%) 1.7			1.4			1.2			1.0			0.8			0.6			0.4		
	E_0	$\Delta E'$	$\frac{\Delta E'}{\Delta\epsilon}$ (×10^2)	E_0	$\Delta E'$	$\frac{\Delta E'}{\Delta\epsilon}$ (×10^2)	E_0	$\Delta E'$	$\frac{\Delta E'}{\Delta\epsilon}$ (×10^2)	E_0	$\Delta E'$	$\frac{\Delta E'}{\Delta\epsilon}$ (×10^2)	E_0	$\Delta E'$	$\frac{\Delta E'}{\Delta\epsilon}$ (×10^2)	E_0	$\Delta E'$	$\frac{\Delta E'}{\Delta\epsilon}$ (×10^2)	E_0	$\Delta E'$	$\frac{\Delta E'}{\Delta\epsilon}$ (×10^2)
31	4.54	0.774	0.46	4.61	0.568	0.41	4.53	0.47	0.40	4.90	0.35	0.35	4.82	0.20	0.25	4.85	0.17	0.29	4.75	0.14	.35
50	4.24	0.642	0.38	4.46	0.544	0.39	4.42	0.41	0.34	4.59	0.34	0.34	4.53	0.20	0.25	4.58	0.16	0.27	4.59	0.13	.33
75	3.93	0.509	0.23	3.90	0.513	0.37	3.89	0.39	0.33	3.62	0.19	0.19	3.63	0.17	0.21	3.63	0.21	0.34	3.65	0.06	.16
110	2.84	0.606	0.36	2.97	0.474	0.34	2.92	0.41	0.34	2.12	0.21	0.21	2.11	0.16	0.20	2.17	0.11	0.19	2.13	0.08	.20
125	2.60	0.540	0.32	2.64	0.438	0.31	2.60	0.38	0.31	1.85	0.20	0.20	1.86	0.16	0.20	1.85	0.11	0.19	1.93	0.09	.22
140	2.29	0.505	0.30	2.30	0.428	0.31	2.40	0.37	0.30	1.63	0.17	0.17	1.71	0.15	0.19	1.68	0.12	0.20	1.72	0.085	.21

TABLE X
Values of E_0 and $\Delta E'$ (in dyn/cm^2) and $\Delta E'/\Delta\epsilon$ Nylon 66 Monofil

Temperature (°C)	$\Delta\epsilon$ (%) 1.0			0.8			0.6			0.4			0.3		
	E_0	$\Delta E'$	$\Delta E'/\Delta\epsilon$ ($\times 10^2$)	E_0	$\Delta E'$	$\Delta E'/\Delta\epsilon$ ($\times 10^2$)	E_0	$\Delta E'$	$\Delta E'/\Delta\epsilon$ ($\times 10^2$)	E_0	$\Delta E'$	$\Delta E'/\Delta\epsilon$ ($\times 10^2$)	E_0	$\Delta E'$	$\Delta E'/\Delta\epsilon$ ($\times 10^2$)
30	5.95	0.83	0.83	5.90	0.65	0.81	5.90	0.53	0.81	6.45	0.43	1.08	6.45	0.28	0.93
55	5.70	0.70	0.70	5.70	0.58	0.73	5.50	0.47	0.78	6.05	0.42	1.05	6.10	0.35	1.17
80	5.25	0.65	0.65	5.05	0.57	0.71	5.10	0.42	0.70	5.50	0.42	1.05	5.55	0.30	1.00
105	4.30	0.55	0.55	4.45	0.50	0.63	4.45	0.42	0.70	4.90	0.30	0.75	4.90	0.27	0.90
120	4.05	0.60	0.60	4.00	0.50	0.63	4.00	0.38	0.63	4.30	0.30	0.75	4.25	0.25	0.83
135	3.60	0.51	0.51	3.70	0.45	0.56	3.65	0.38	0.63	3.90	0.28	0.70	3.90	0.18	0.60
160	3.00	0.45	0.45	3.15	0.37	0.46	3.20	0.37	0.62	3.30	0.25	0.63	3.30	0.20	0.67

TABLE XI
Values of E_0 and $\Delta E'$ (in dyn/cm^2) and $\Delta E'/\Delta\epsilon$, Nylon 12 Monofil

Temperature (°C)	$\Delta\epsilon$ (%) 1.2			1.0			0.8			0.6		
	E_0	$\Delta E'$	$\Delta E'/\Delta\epsilon$ ($\times 10^2$)	E_0	$\Delta E'$	$\Delta E'/\Delta\epsilon$ ($\times 10^2$)	E_0	$\Delta E'$	$\Delta E'/\Delta\epsilon$ ($\times 10^2$)	E_0	$\Delta E'$	$\Delta E'/\Delta\epsilon$ ($\times 10^2$)
40	7.19	1.36	1.13	6.15	1.06	1.06	6.38	0.77	0.96	6.50	0.65	1.08
60	6.52	1.29	1.08	5.61	0.98	0.98	5.91	0.82	1.02	5.86	0.54	0.90
80	5.74	1.06	0.88	4.98	0.83	0.83	5.08	0.66	0.83	4.87	0.52	0.87
95	5.22	0.99	0.82	4.49	0.78	0.78	4.61	0.59	0.74	4.26	0.52	0.87
115	4.47	0.87	0.73	4.16	0.71	0.71	4.02	0.48	0.60	3.78	0.35	0.58
130	4.02	0.82	0.68	3.78	0.53	0.53	3.66	0.46	0.58	3.45	0.34	0.57

correlation between the average dynamic modulus expressed above and the changes in modulus during the cycle measured by a high-frequency cyclic experiment. $E(0)$ and $\Delta E'/\Delta\epsilon$ increase with increasing orientation as indicated by the data of low- and high-draw-ratio nylon 6 fiber.

Nonlinear Elastic Stress $\sigma_{el}(\theta)$

The determination of $\sigma_{el}(\theta)$ is an important step in this analysis because it provides the reference for calculating the phase angle difference $\delta(\theta)$. Note that $\sigma_{el}(\theta)$ represents the response of a nonlinear elastic body (i.e., a body exhibiting no loss) to the sinusoidal strain, with the modulus of material changing during the cycle.

Since $\sigma_{el}(\theta)$ is directly related to $E(\theta)$, deviation from linear behavior can be estimated from the data in Tables VIII–XI. Both $\Delta E'$ and $\Delta E'/\Delta\epsilon$ values have physical significance. $\Delta E'$ is proportional to deviation in stress from linear response while $\Delta E'/\Delta\epsilon$ expresses the nonlinearity normalized to a unit strain amplitude. As expected, the fibers become increasingly more nonlinear elastic with increasing strain amplitude. Comparison of low-draw-ratio and high-draw-ratio nylon 6 fibers shows that nonlinearity in elastic stress increases with increasing orientation. However, the difference in $\Delta E'/\Delta\epsilon$ for fully drawn nylon 6, nylon 12, and nylon 66 cannot be attributed to the differences in orientation function of these fibers because with the nylon 66, which has the highest value of orientation function, the nonlinearity in elastic stress is less than that of both nylon 6 and nylon 12, where the degree of orientation is less.

Changes in the Phase Angle Difference During the Cycle

Linear viscoelastic materials exhibit internal friction which is constant during the cycle, and this is reflected by the constant phase angle difference δ. For the nonlinear material, internal friction can be expressed by the variable phase angle difference $\delta(\theta)$ using the nonlinear elastic stress response given by eq. (6) as the reference:

$$\sigma_{el}[\theta + \delta(\theta)] = \sigma_{exp}\ (\theta) \tag{12}$$

Thus, it should be noted that $\delta(\theta)$ signifies the phase lag between the nonlinear elastic stress and the viscoelastic stress as derived from eqs. (6) and (12).

Plots of $\delta(\theta)$ for nylon 6 fibers at 25, 90, and 150°C are presented in Figures 10(a)–10(c).

With all fibers and under all testing conditions, $\delta(\theta)$ exhibits two distinct maxima, one near $\theta = 0°$ and the other near $\theta = 180°$ (see Fig. 11). The minima of $\delta(\theta)$ lie near 270° and 90°. Maxima in $\delta(\theta)$ occur at the values of θ where the deformation rate during the cycle is at maximum. We speculated that at large strain amplitudes the internal friction at a given value of θ and thus $\delta(\theta)$ is dependent on the rate of deformation during the cycle. Experiment at constant deformation rate and same total displacement proved that this is the case. With constant deformation rate $\delta(\theta)$ is constant during the extension and during contraction, but δ in extension may be different from δ in contraction because of the effects associated with strain-induced structural changes discussed below.

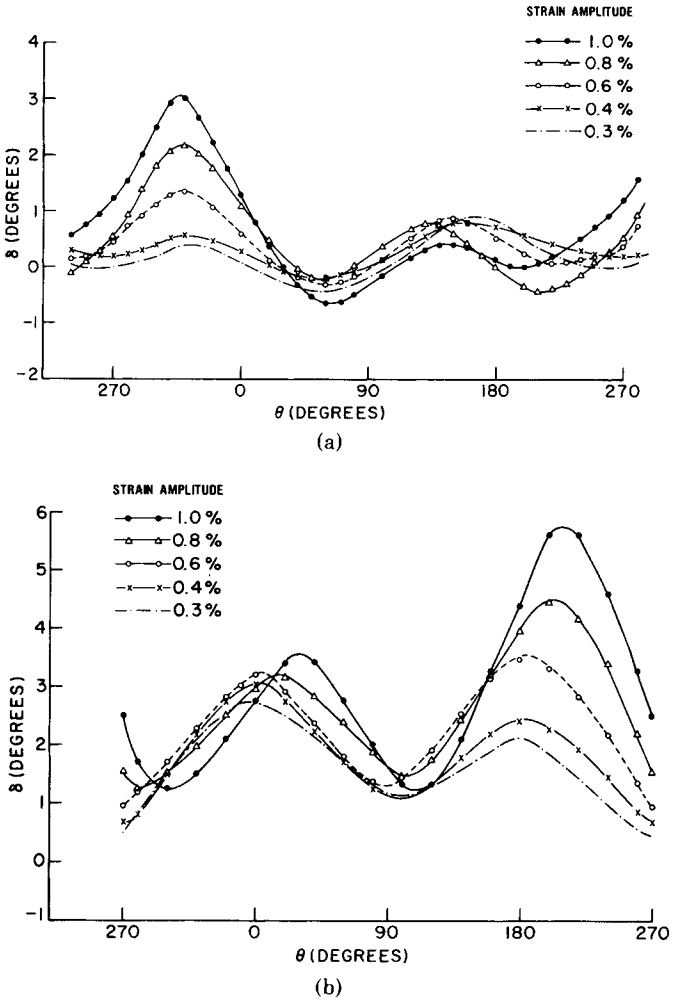

Fig. 10. $\delta(\theta)$ of nylon 6 fibers, (a) 25°C, (b) 90°C, (c) 150°C.

The behavior of nylon 66 and other fibers is similar in the effect of deformation rate on δ. However, changes in $\delta(\theta)$ with temperatures and strain amplitude follow different patterns. For comparison, we present the data of $\delta(\theta)$ for nylon 66 at 60, 105, 135, and 160°C in Figure 11. More pronounced than in the case of nylon 6 is the difference in the minima in $\delta(\theta)$ at 90° and 270°. In most cases, the value of $\delta(270°)$ is considerably higher than that of $\delta(90°)$.

The fact that average value of δ in extension is often different from δ in contraction is attributed to the reversible strain-induced structural changes occurring during the cycle. The presented data allow the estimation of the energies associated with these reversible strain-induced structural changes, which in turn provide the information regarding the nature of the strain-induced structural change.[2]

In analogy to the linear viscoelastic solids where the loss per cycle is given by

$$\xi = \pi E \Delta\epsilon^2 \sin \delta$$

we calculate the loss in extension and contraction using

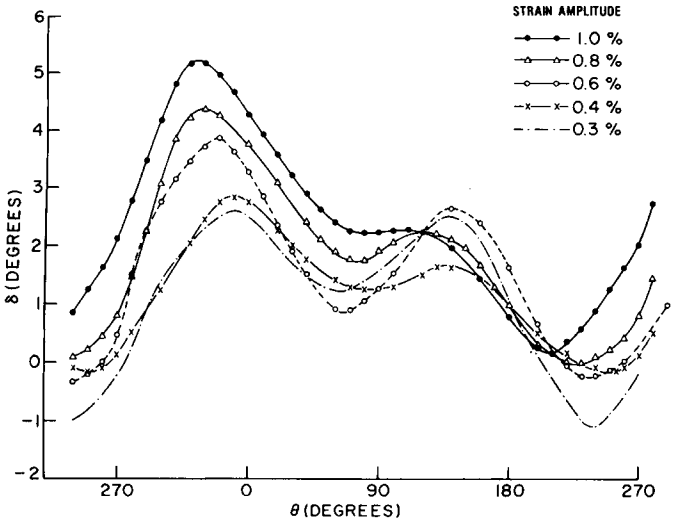

(c)

Fig. 10. (*Continued from previous page.*)

$$\xi = \pi \overline{E}\, \Delta\epsilon^2 \sin \bar{\delta}$$

where $\overline{E}$ and $\bar{\delta}$ are average values of E and δ during extension and contraction. This quantity is discussed in detail in the section following.

Energies Associated with Reversible Strain-Induced Structural Changes

The most interesting variable in the above analysis is the energy associated with the reversible strain-induced structural change (ERSISC). Since it indicates both the magnitude and type of stress-induced structural change during the cycle, we believe that the determination of ERSISC will become a very useful tool in the interpretation of fracture and fatigue of polymeric materials.

In the interpretations of ERSISC data the following points must be remembered:

(1) Energy released in extension and absorbed in contraction represent structural changes that may involve strain-induced orientation, crystallization, improvement in order, closure of longitudinal cracks, or increase in density under stress.

(2) Energy absorbed in extension and released in contraction indicates structural changes which may involve opening of cracks under stress, cavitation, volume expansion, etc.

(3) It is unlikely that conditions would be encountered whereby the strain-induced structural change would involve only the processes classified under (1) or (2). In most cases, we expect that both types of processes would occur simultaneously. Since our analysis yields only the net effect, we can only conclude as to what the overriding mechanisms in each specific case are.

Strain-Induced Reversible Structural Changes in Fully Drawn Fibers

With nylon 6, the effects associated with the reversible strain-induced structural change become significant at strain amplitudes exceeding 0.5% [see Fig. 12(a)]. At temperatures below T_g −30°C and above T_g +30°C, the structural change is such that the energy is absorbed in extension and released in contraction. In the temperature interval between 50 and 130°C, the opposite is the case: the energy is released in extension and absorbed in contraction.

Nylon 12 fibers show a similar behavior, i.e., a well-defined minimum in ERSISC is observed at about 90°C [Fig. 12(c)]. However, with this fiber, positive values of strain-induced energies are observed only at relatively low strain amplitudes. By increasing the strain amplitude, the curves are shifted to lower values which suggests that the orientation or crystallization effect is overriding and that the extent of increase in order increases with increasing strain amplitude.

Strain-induced structural changes in nylon 66 becomes significant at strain amplitudes exceeding 0.5% [Fig. 12(b)]. The curves exhibit a minimum at about 100°C. In all cases, the energy is absorbed in extension and released in contraction. In contrast with nylon 6 and nylon 12, the values of ERSISC become more positive with increasing strain amplitude. This suggests that crack opening and cavitation effects are the main factors in ERSISC.

The data discussed above lead to the following conclusions with regard to the effect of strain amplitude and temperature on ERSISC:

(1) Strain amplitude at which ERSISC has a significant effect on the shape of the hysteresis loop is about 0.5%.

(2) With all fully drawn polyamide fibers, values of ERSISC go through a well-defined minimum at about 95°C which corresponds to the glass transition temperature of these fibers.

(3) Absolute values of ERSISC increase with increasing strain amplitude.

(4) With nylon 6 and nylon 12, ERSISC becomes progressively more negative with increasing strain amplitude. Note that with nylon 6, this trend is restricted to the temperature range between T_g − 30°C and T_g + 30°C.

(5) With nylon 66, increasing strain amplitude leads to positive increase in ERSISC. The same trend is observed with nylon 6 outside the T_g − 30°C to T_g + 30°C temperature interval.

With regard to the interpretation of these data, there is an important point to note in the results of nylon 6. Note that at all strain amplitudes, values of ERSISC remain close to zero at 50 and 130°C, while below and above these two temperatures, they either increase or decrease monotonically with increasing strain amplitude. It is very unlikely that strain-induced structural changes do not occur at these two temperatures, while they are significant both below and above these temperatures. Therefore, we believe that these data should be interpreted as indicating that at these two temperatures the two effects (i.e., ordering and cavitation) nearly cancel each other.

The ordering effects on the basis of the above results are most pronounced at temperatures near T_g. This holds for all of these fibers. With decreasing and increasing of the testing temperatures, the effects associated with cavitation, dilation, etc., become more and more pronounced.

It is obvious that nylon 66 whose ERSISC values are always positive represents an exceptional case in which the cavitational effect is always predominant.

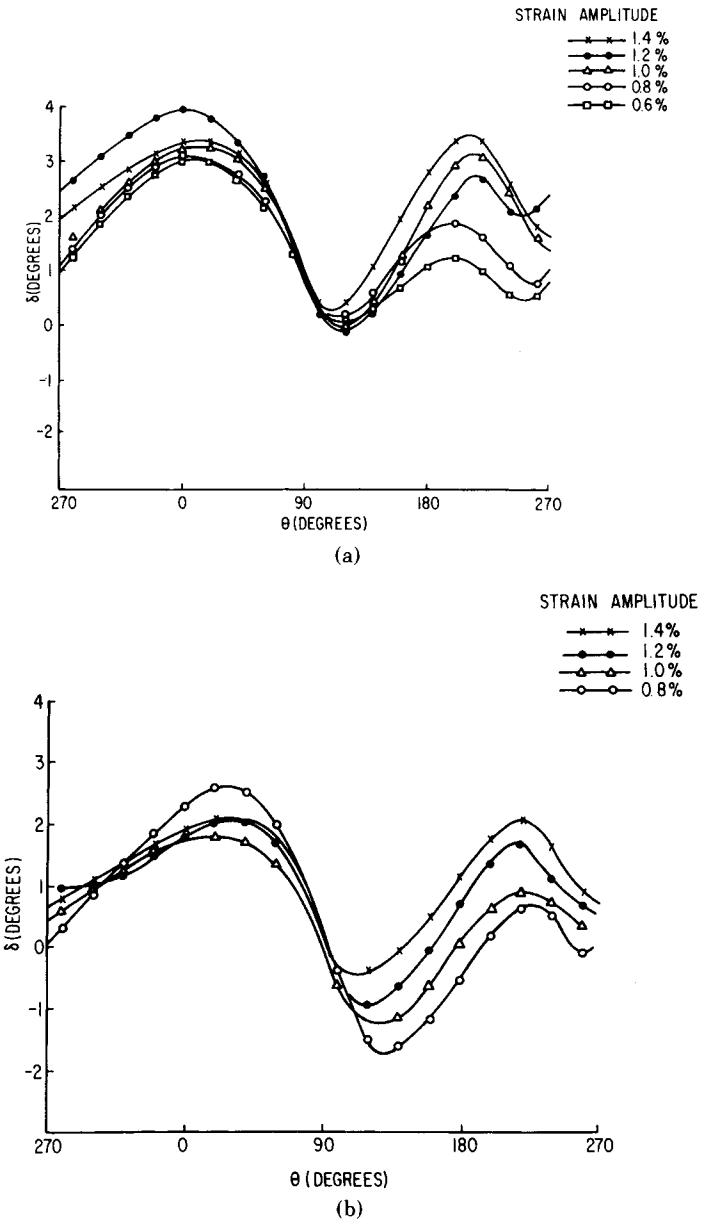

Fig. 11. $\delta(\theta)$ of nylon 66 fibers, (a) 60°C, (b) 105°C, (c) 135°C, (d) 160°C.

In the first approximation, it is reasonable to assume that, with similar morphologies, the relative effects of orientation in ERSISC should decrease with increasing orientation of the samples. Thus, a perfectly oriented sample should undergo primarily dilational and crack opening changes during mechanical straining. This hypothesis seems to be supported by the x-ray data. Note that at 1% strain amplitude the values of ERSISC at 100°C increase from −3 with nylon 12 to +1.5 with nylon 66, while the corresponding orientation function increases from 0.88 to 0.97 (as follows):

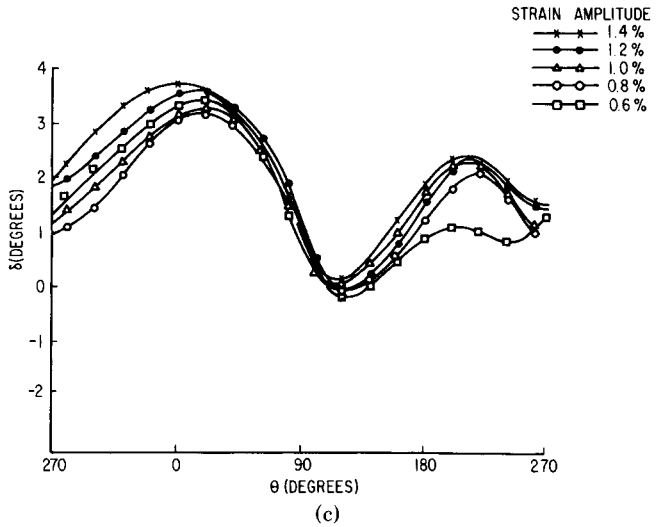

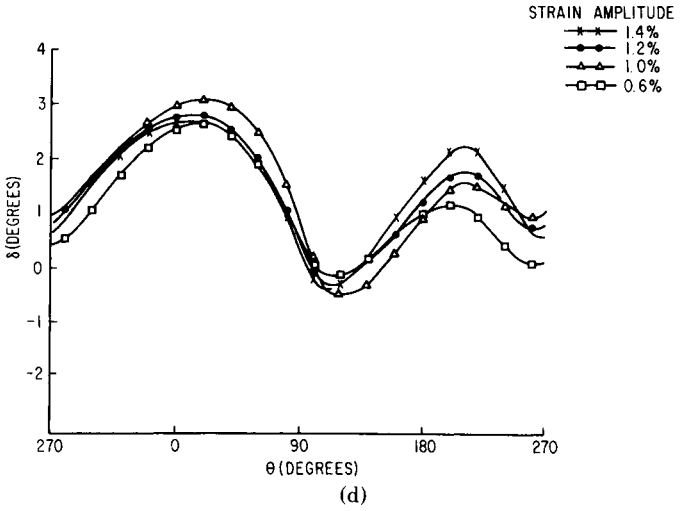

Fig. 11. (*Continued from previous page.*)

Fiber	*ERSISC value*	*Orientation function*
nylon 66	+1.5	0.97
nylon 6	−2	0.945
nylon 12	−3	0.88

It is obvious that factors other than orientation function may have a role in the response of a fiber under stress. However, the indicated relationship can readily be explained, and therefore the observed relationship between orientation function and ERSISC may be coincidental.

Since the data of Figure 12 were obtained with three different fibers, it was desirable to establish the effect of orientation on ERSISC with the fibers made from the same polymer but different draw ratio (orientation function). For this

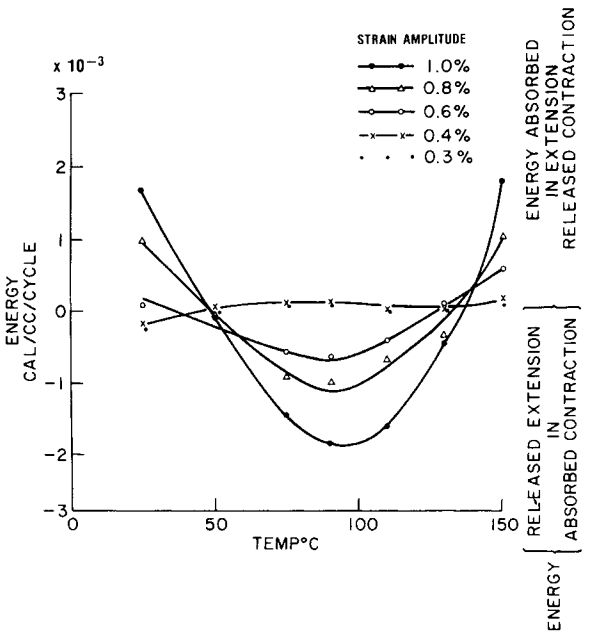

(a)

purpose, we analyzed the dynamic properties of a nylon 6 fiber of draw ratio $3x$.

Plots of ERSISC versus temperature for nylon 6 fiber of draw ratio 3 are pre-

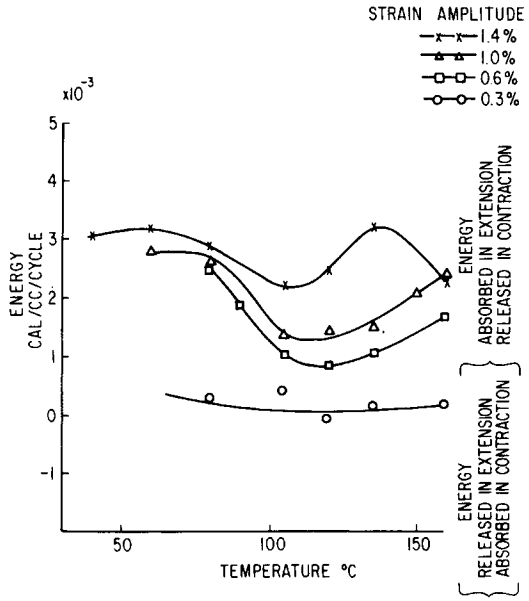

(b)

Fig. 12. Effect of strain amplitude and temperature on energy of strain-induced structural changes (a) nylon 6, (b) nylon 66, (c) nylon 12.

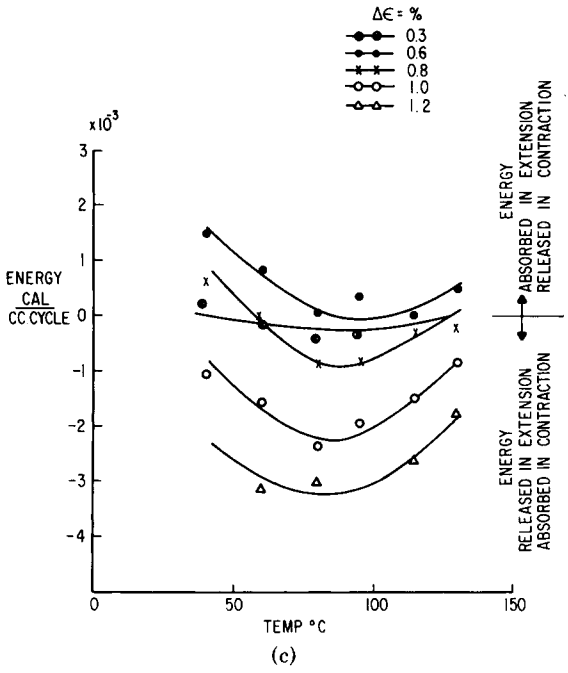

(c)

Fig. 12. (*Continued from previous page.*)

sented in Figure 13. In contrast with nylon 6 of draw ratio 5.3x, this low draw ratio fiber has negative ERSISC values over the entire temperature range (30–150°C).

A secondary minimum is indicated at ~90°C and the values decrease with

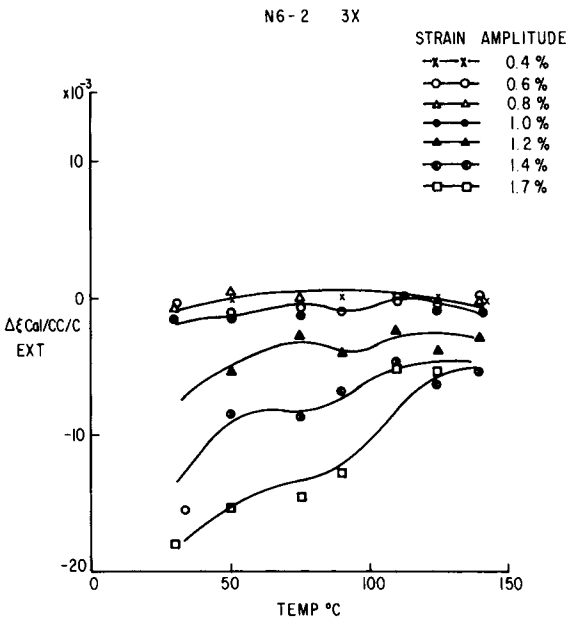

Fig. 13. ERSISC vs. temperature, nylon 6, 3x.

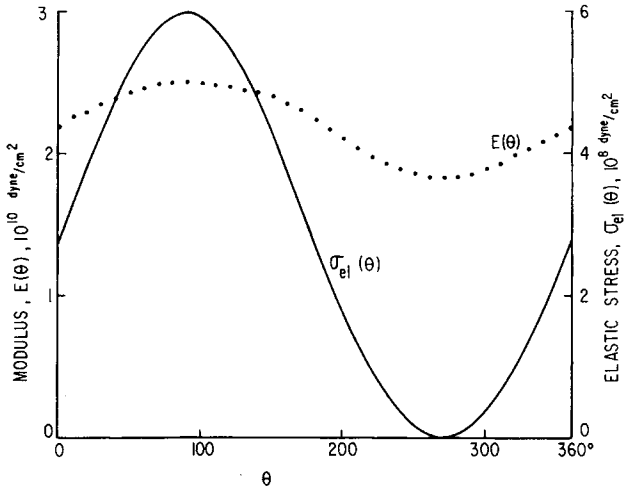

Fig. 14. Modulus and elastic stress, nylon 6, $3x$, $\Delta\epsilon = 1.2\%$, 140°C.

increasing strain amplitude. The most important point, however, is the magnitude of ERSISC, which may be as low as −18 with the fiber drawn at $3x$, while the lowest value recorded with the fiber drawn at $5.3x$ is only −2. These results, therefore, support the assumption that orientation has an important role in the sign and magnitude of ERSISC and that the general trend is that values of ERSISC increase positively with increasing orientation.

With low-orientation fibers, ERSISC is negative which indicates that orientation and crystallization effect during stretching control the shape of the hysteresis loop. With increasing orientation, the values of ERSISC increase and may become positive, which indicates that cavitation becomes the overriding factor.

SUMMARY AND CONCLUSIONS

The purpose of this study was to develop a method to characterize the nonlinear response in cyclic straining of nylon 6, nylon 66, and nylon 12 fibers. The upper limit of the strain amplitude approached conditions at which fatigue failure was observed during the experiments. It is therefore expected that the presented data will help to establish a link between the viscoelastic properties and time to failure under cyclic loading. In most cases, the cyclic loading is so severe that the sample undergoes considerable structural and property changes during the

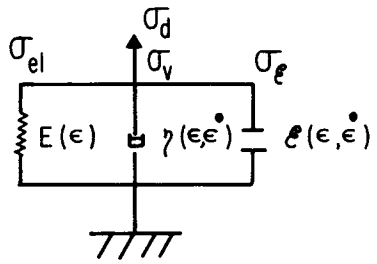

Fig. 15. Three-element Voigt model.

experiment, a phenomenon which is frequently referred to as mechanical conditioning. Unless the deformation is very severe, the samples subjected to strain amplitudes exceeding 0.2% reach a steady state at which the role of property change becomes negligible almost to the moment of rupture. The present study concerns primarily the data analysis obtained at such steady-state conditions.

The data are analyzed in terms of (1) average properties, i.e., mechanical loss and apparent dynamic modulus, and (2) property changes during the cycle. This latter analysis includes determination of instantaneous modulus and instantaneous phase angle difference between the elastic stress and viscoelastic stress, i.e., $E(\theta)$ and $\delta(\theta)$, as well as the calculation of the energy associated with the strain-induced structural change. The described analysis of property changes during the cycle provides an interpretation for the distortion of the stress resulting from a sinusoidal strain.

In comparing the data of fully drawn nylon 6, nylon 66, and nylon 12 fibers, we observed several trends which are common to all of these fibers. This includes a decrease in apparent modulus and increase in mechanical loss with increasing strain amplitude. Similarly, all fibers exhibit a decrease in the temperature of maximum loss with increasing strain amplitude.

In quantitative terms, the responses are different. For example, nylon 6 shows the largest drop in modulus with increasing strain amplitude while nylon 66 exhibits a large increase in loss with increasing strain amplitude. Differences exist also in the shifts in the temperature of maximum loss with strain amplitude. Comparison of low- and high-draw-ratio nylon 6 indicates that morphology is an important factor in these average viscoelastic properties.

With regard to the changes in properties during the cycle, we found that (1) average modulus $E(0)$ and (2) changes in modulus with strain $dE/d\epsilon$ decrease with increasing temperature and increasing strain amplitude. In addition, $E(\theta)$ which at small strain amplitudes can sometimes be approximated by sinusoidal approximation of

$$E(\theta) = E_0 + \Delta E \sin \theta$$

becomes more complex with increasing strain amplitude.

The nonlinearity in elastic stress increases with increasing strain amplitude and increasing orientation. However, there are significant differences among the behavior of nylon 6, nylon 66, and nylon 12. Of the three fibers, the nonlinearity in elastic stress is smallest with nylon 66.

The angular dependence of phase angle difference $\delta(\theta)$ of all fibers is similar in the appearance to two maxima, one at $\sim 0°$ and the other at $\sim 180°$. Experiments under constant deformation rate showed that these two maxima must be attributed primarily to the effect of deformation rate on δ. In most cases, the average $\bar{\delta}$ in extension differs from $\bar{\delta}$ in contraction. These indicate that fibers undergo reversible strain-induced structural change during each cycle. Based on the sign and magnitude of these energies, it is possible to establish the type of structural changes which has an overriding role in these effects.

One important difference between nylon 6 and nylon 66 is that at temperatures between 50 and 130°C nylon 6 releases energy in extension and absorbs energy in contraction. Such energy effects are attributed to strain-induced crystallization or orientation, reversible increases in order, etc. With nylon 66, on the other hand, the most important mechanism appears to be opening of the crack

or cavitation. The orientation effects increase with decreasing orientation as indicated by the data of low- and high-draw-ratio nylon 6 fibers.

In contrast with the harmonic analysis, which helps reproduce the shape of stress (strain) resulting from the sinusoidal strain (stress), the interpretive analysis allows the determination of causes for the distortions. We hope that this method will contribute to improve our understanding of the behavior of polymeric materials subjected to stresses or strains encountered in actual practices.

The results presented in this article provide the basis for a morphological hypothesis to explain the superior mechanical behavior of nylon 6 as compared to nylon 66. The viscoelastic data discussed above can be explained if one assumes that the dilation of nylon 6 under stress is more uniform throughout the volume of fiber than in nylon 66. This could be a result of a higher amount of tie molecules (i.e., chain folding) between crystalline and amorphous domains, or a difference in the response of crystalline phase under stress. With regard to this latter effect, the results suggest that under stress the crystal lattice of nylon 6 expands more than that of nylon 66. The net effect is a higher tendency of nylon 66 to form cracks under stress, while in nylon 6 the stress results in higher alignment of molecules and crystallites. A higher decrease in T_g with strain amplitude observed with nylon 66 is consistent with these interpretations.

APPENDIX A

Proportionality Constant k in the Normalization Procedure of Elastic Stress

In the calculation of the nonlinear elastic stress, we assume that the instantaneous modulus during the cycle, $E(\theta)$ is proportional to the ratio of stress amplitude to strain amplitude of the superimposed wave at the same value of θ. This leads to

$$E(\theta) = k(\Delta\sigma_s/\Delta\epsilon_s)$$

The normalization procedure involves the evaluation of k in

$$\Delta\sigma_{\text{exp}} \cos \delta(90°) = k \int_{3\pi/2}^{\pi/2} (\Delta\sigma_s/\Delta\epsilon_s)_\theta \Delta\epsilon \cos\theta \, d\theta$$

Considering the above relation, one realizes that the value of k is affected by two factors: (1) the frequency dependence of modulus, and (2) the internal friction of the material as reflected by $\cos \delta(90°)$.

The frequency dependence of modulus is the result of the difference in frequency between the high-frequency superimposed strain and the fundamental strain for which $E(\theta)$ is being determined.

With materials having very low loss this effect should determine the value of k. Since the modulus of these fibers in general increases with frequency, it is expected that under these conditions, k should be less than one. If, however, the loss becomes very large, the left-hand term including $\cos \delta(90°)$ may become important which in turn should lead to an increase in k. In order to verify this hypothesis, we examined values of k determined in these studies and found a gratifying agreement between observed and expected trends. For illustration, we present in Tables A-1 and A-2 the data of k determined for the low modulus nylon 6 and nylon 12. With nylon 12, k is less than 1 for all experimental conditions. Its value decreases with increasing temperatures and decreasing strain amplitude. The loss of nylon 12 fibers is under all conditions below 0.2 cal/cm^3/sec. With low-draw-ratio nylon 6, on the other hand, k values are either greater or smaller than one, depending on the severity of testing conditions [i.e., the magnitude of strain amplitude $(\Delta\epsilon)$].

With strain amplitudes $\Delta\epsilon \geq 1.2\%$, $k > 1$, while with strain amplitudes $\Delta\epsilon \leq 1.0$, $k < 1$. An inspection of loss data for the low-draw-ratio nylon 6 shows that with $\Delta\epsilon \geq 1.2$, the losses are much

TABLE A-1
Values of K Factor Nylon 6 (3x), Monofil

	$\Delta\epsilon$ (%)													
	1.7		1.4		1.2		1.0		0.8		0.6		0.4	
$\Delta E/\Delta\epsilon$ T (°C)	$\Delta E/\Delta\epsilon$ ($\times 10^2$)	K	$\Delta E/\Delta\epsilon$ ($\times 10^2$)	K	$\Delta E/\Delta\epsilon$ ($\times 10^2$)	K	$\Delta E/\Delta\epsilon$ ($\times 10^2$)	K	$\Delta E/\Delta\epsilon$ ($\times 10^2$)	K	$\Delta E/\Delta\epsilon$ ($\times 10^2$)	K	$\Delta E/\Delta\epsilon$ ($\times 10^2$)	K
30	0.46	1.23	0.41		0.40		0.35	0.953	0.25	0.962	0.29	0.979	0.35	
50	0.38	1.10	0.39	1.18	0.34	1.27	0.34	0.916	0.25	0.948	0.27	0.986	0.33	0.997
75	0.23	0.959	0.37	1.05	0.33	1.15	0.19	0.817	0.21	0.872	0.34	0.942	0.16	1.01
110	0.36	1.09	0.34	1.11	0.34	1.15	0.21	0.891	0.20	0.917	0.19	0.902	0.20	0.948
125	0.32	1.10	0.31	1.12	0.31	1.18	0.20	0.90	0.20	0.917	0.19	0.928	0.22	0.923
140	0.30	1.09	0.31	1.14	0.30	1.14	0.17	0.88	0.19	0.906	0.20	0.902	0.21	0.912

TABLE A-2
Values of K Factor Nylon 12, Monofil

T (°C)	$\Delta\dot{\epsilon}$ (%) 1.2	1.0	0.8	0.6
40	0.764	0.891	0.909	0.928
60	0.751	0.860	0.880	0.918
80	0.732	0.838	0.868	0.907
95	0.737	0.811	0.833	0.891
115	0.761	0.752	0.814	0.855
130	0.733	0.744	0.797	0.846

higher and reach 600 cal/cm^3/sec at $\Delta\epsilon = 1.7\%$. Thus, it can be concluded that k is indeed controlled by the difference in the frequency between the superimposed and fundamental wave and the magnitude of the loss.

APPENDIX B

Example of the Calculation of Nonlinear Elastic Stress from the Modulus that was Measured as a Function of Strain during a Cycle

The nonlinear elastic modulus that varies with the strain is measured by superimposing a high-frequency small-amplitude cyclic strain. The modulus $E(\theta)$ or $E(\epsilon)$ is used to calculate the elastic stress σ_{el} as follows:

$$\sigma_{el}(\epsilon) = \sigma_{el}(\epsilon_{ref}) + \int_{\epsilon_{ref}}^{\epsilon} E(\epsilon)\, d\epsilon \tag{B-1}$$

or

$$\sigma_{el}(\theta) = \sigma_{el}(\theta_{ref}) + \int_{\theta_{ref}}^{\theta} E(\theta) \cdot \Delta\epsilon \cos\theta\, d\theta \tag{B-2}$$

In eqs. (B-1) and (B-2), the subscript "ref" indicates a reference point. A convenient reference point is the minimum strain point, i.e., $\theta = 270°$.

Figure 14 shows an example of $E(\theta)$ and $\sigma_{el}(\theta)$ for the case of nylon 6 (draw ratio 3) sample with $\Delta\epsilon = 1.2\%$ at 140°C.

APPENDIX C

Relationship Between Nonlinear Elastic Stress and Nonlinear Viscoelastic Stress

The phase angle difference $\delta(\theta)$, which relfects the change in loss during the cycle, is obtained using the following expression:

$$\sigma_{el}[\theta + \delta(\theta)] = \sigma_{exp}(\theta)$$

correlating the nonlinear elastic stress $\sigma_{el}(\theta)$ and the experimentally determined viscoelastic stress $\sigma_{exp}(\theta)$..

In general, the peak-to-peak difference of the nonlinear viscoelastic stress should be higher than that of the nonlinear elastic stress $\sigma_{el}(\theta)$. Here, $\sigma_{el}(\theta)$ represents the stress of a nonlinear elastic body whose modulus change during the cycle is equal to the modulus change during the cycle $E(\theta)$ determined by (1) high-frequency superimposition experiment and (2) normalization procedure involving the following relation:

$$(\sigma_{max} - \sigma_{min}) = \int_{3\pi/2}^{\pi/2} E(\theta)\Delta\epsilon \cos\theta\, d\theta$$

$$= \int_{3\pi/2}^{-/2} k(\Delta\sigma_s/\Delta\epsilon_s)_\theta\, \Delta\epsilon \cos\theta\, d\theta$$

Here we show that $\Delta\sigma_{el}$ can be approximated by

$$\Delta\sigma_{el} = \Delta\sigma_{exp} \cos \delta_{90°} \tag{C-1}$$

where $\Delta\sigma_{el}$ is the amplitude of elastic stress in sinusoidal straining, $\Delta\sigma_{exp}$ is the amplitude of viscoelastic stress in sinusoidal straining, and $\delta_{90°}$ is the elastic stress–viscoelastic stress phase angle difference at $\theta = 90°$.

In linear case, eq. (C-1) holds by definition. In nonlinear case, numerical experiments show that it holds approximately.

The need for the relation of eq. (C-1) arises in the consideration of the dynamic nonlinear viscoelasticity under sinusoidal straining where we need the concept of elastic stress versus viscoelastic stress.

In order to estimate the elastic stress, we carry out the "strain superimposition" experiment to determine the variation of modulus with the strain. The resulting modulus was found to vary with the strain. Thus, we encounter a problem of uncertainty as to the proper way of establishing the elastic stress.

First, let us consider the linear case. If a specimen is subjected to a sinusoidal strain of

$$\epsilon(\theta) = \epsilon_0 + \Delta\epsilon \sin\theta \tag{C-2}$$

the stress response is

$$\sigma_d(\theta) = \sigma_0 + \Delta\sigma_d \sin(\theta + \delta) \tag{C-3}$$

The storage modulus which is the elastic modulus is given by

$$E' = (\Delta\sigma_d/\Delta\epsilon) \cos \delta \tag{C-4}$$

and the elastic stress during the cycle at a phase angle θ is obtained by the integration of E' with respect to the strain, i.e.,

$$\begin{aligned}\sigma_{el}(\theta) &= \sigma_0 + \int_0^\theta E' \, d\epsilon \\ &= \sigma_0 + E' \, \Delta\epsilon \sin \theta\end{aligned} \tag{C-5}$$

Thus, $\Delta\sigma_{el}$ in this case is equal to $E' \, \Delta\epsilon$ and by comparing eqs. (C-4) and (C-5),

$$\Delta\sigma_{el} = \Delta\sigma_{exp} \cos \delta = \Delta\sigma_{exp} \cos \delta_{90°} \tag{C-6}$$

because δ is constant in linear case.

Now, for the nonlinear case, we resort to the following numerical experiments in deducing eq. (C-1). For this purpose, we consider the modified Voigt model with three elements shown in Figure 15.

This model is based on the findings of the nonlinear dynamic behavior of the fibers as discussed in this article. The spring and dashpot are dependent on the strain and strain rate, and the third element reflects the energy effect of the strain-induced structural change. Considering the dynamic behavior of the fibers in sinusoidal straining, we represent each of the three elements as follows:

$$E(\epsilon) = E_0 + E_0 e' (\epsilon - \epsilon_0)$$

or

TABLE A-3
Numerical Experiments to Check Equation (C-1)[a]

Run No.	Parameters				$\Delta\sigma_{el}/\Delta\sigma_{exp}$	cos $\delta_{90°}$	$\delta_{90°}$
	e	η_0, 10^9	b	d			
1	0	0.2	0	0	0.97	0.97	14.1
2	0	0.4	0	0	0.894	0.894	26.7
3	0.15	0.2	0	0	0.969	0.977	12.3
4	0.15	0.2	0.2×10^9	0	0.956	0.969	14.2
5	0.15	0.2	0.2×10^9	0.4×10^9	0.976	0.982	−10.9
6	0	0.2	0	0.4×10^9	0.97	0.97	−14.1
7	0	0.2	0.2×10^9	0	0.958	0.958	16.7

[a] $E_0 = 0.5 \times 10^{11}$; $\epsilon_0 = 0.01$; $\Delta\epsilon = 0.01$; $\omega = 62.8$; $\sigma_0 = 0.1 \times 10^{10}$; $a = 0$; $c = 0$.

$$E(\theta) = E_0 + \epsilon_0 e \sin\theta \tag{C-7}$$

$$\eta(\epsilon,\dot{\epsilon}) = \eta_0 + a\epsilon + b|\dot{\epsilon}| \tag{C-8}$$

$$d\mathcal{E}(\epsilon) = (c - d\dot{\epsilon})\, d\epsilon$$

or

$$\sigma_{\mathcal{E}} = d\mathcal{E}(\epsilon)/d\epsilon = c - d\dot{\epsilon} \tag{C-9}$$

In these equations, e', e, a, b, c, and d are constants, $\mathcal{E}$ represents the energies associated with the strain-induced structural changes, and the superscript dot indicates the time rate.

Then, the stress response to a sinusoidal straining of eq. (C-2) is

$$\sigma_{\text{exp}}(\theta) = \sigma_{\text{el}}(\theta) + \sigma_v(\theta) + \sigma_{\mathcal{E}}(\theta) \tag{C-10}$$

$$\sigma_{\text{el}}(\theta) = \sigma_0 + \Delta\epsilon(E_0 \sin\theta + 0.5E_0 e \sin^2\theta) \tag{C-11}$$

$$\begin{aligned}\sigma_v(\theta) &= \eta(\theta)\,\dot{\epsilon} \\ &= (\omega\Delta\epsilon\cos\theta)\,(\eta_0 + a\epsilon + b\omega\,\Delta\epsilon|\cos\theta|)\end{aligned} \tag{C-12}$$

$$\sigma_{\mathcal{E}}(\theta) = c - d\,\omega\Delta\epsilon\cos\theta \tag{C-13}$$

With this assumption we carried out numerical experiments. Results are shown in Table A-3. The results show that eq. (C-1) holds approximately even for cases in which the phase angle difference between the elastic stress and viscoelastic stress is fairly large.

References

1. Y. D. Kwon, R. K. Sharma, and D. C. Prevorsek, *Adv. Chem. Ser., No. 174,* 35 (1979).
2. D. C. Prevorsek, Y. D. Kwon, and R. K. Sharma, *J. Macromol. Sci. Phys.,* **13**(4), 571 (1977).
3. O. Nakada, *J. Phys. Soc. Jpn.,* **15**(12), 2280 (1960).

Received November 13, 1979
Accepted January 22, 1980